Clays and Clay Minerals, Vol. 54, No. 5, 555–570, 2006.

GEOLOGY, MINERALOGY AND ORIGIN OF CLAY MINERALS OF THE PLIOCENE FLUVIAL-LACUSTRINE DEPOSITS IN THE CAPPADOCIAN VOLCANIC PROVINCE, CENTRAL ANATOLIA, TURKEY

ALİ GÜREL[1,*] AND SELAHATTİN KADİR[2]

[1] Niğde University, Department of Geological Engineering, 51200 Niğde, Turkey
[2] Eskişehir Osmangazi University, Department of Geological Engineering, 26480 Meşelik, Eskişehir, Turkey

Abstract—The Güzelöz-İncesu Plateaus are situated in the central and eastern parts of the Cappadocian volcanic province (central Anatolia). This province contains many ignimbrite levels, andesite, basalt intercalated with several paleosols, calcrete, carbonate, fluvial sediments, diatomaceous clayey sediments and pyroclastic sedimentary levels. The presence of mottling, sesquioxide, root traces, rhizoids and burrows in continuous, finely bedded and laminated sediments, paleosols, calcrete, the occurrence of bone- and teeth-bearing reworked pyroclastic materials, and the description of the lithofacies in the study area indicate fluvial and shallow-lake environments. These environments are dominated by smectite and illite, with traces of kaolinite, associated mainly with plagioclase, K-feldspar, quartz, calcite, opal-CT, pyroxene (diopside, rare hypersthene), and locally trace amounts of gypsum and sepiolite. Smectite predominates in paleosols and calcrete units, and generally increases upwards in the profiles, coinciding with a gradual increase in the degree of alteration. Partial to complete alteration of plagioclase, K-feldspar, pyroxene and partial devitrification of glass-shard particles in pyroclastic rocks, development of microsparitic to sparitic cement comprising euhedral rhombic calcite crystals between irregular clay nodules in paleosol and calcrete samples, along with the occurrence of dogtooth-type sparitic crystals in fractures, desiccation cracks and geopetal-type fenestrae, indicate alternating periods of drought and wet, resulting in the development of paleosols and calcretes. Micromorphological development of spongiform smectite on mainly relict feldspar and, locally, on glass shards, indicates an authigenic origin, whereas illite formed either authigenically or by conversion of smectite to illite-smectite.

Key Words—Calcrete, Cappadocian Volcanic Province, Central Anatolia, Clay Minerals, Paleoenvironment, Paleosol, Turkey.

INTRODUCTION

Volcano-sedimentary units underlying the Güzelöz-İncesu Plateaus in the central and eastern parts of the Cappadocian volcanic province (CVP-central Anatolia) comprise intercalations of paleosols, calcretes, carbonates, fluvial sediments, diatomaceous clayey sediments and pyroclastic-sediment levels. These levels are composed of mainly smectite-dominated clay minerals associated with feldspar, pyroxene and glass shards from volcanic units.

To date, the region has been studied mainly for its volcanism, mining geology, mineralogy-petrography and tectonics (Pasquaré, 1968; Pasquaré *et al.*, 1988; Batum 1975, 1978; Innocenti *et al.*, 1975; Besang *et al.*, 1977; Ercan *et al.* 1987, 1989; Göncüoğlu and Toprak 1992; Le Pennec *et al.*, 1994; Duritt *et al.*, 1995; Bigazzi *et al.*, 1997; Schumacher and Schumacher, 1996; Gevrek, 1997; Türkecan *et al.*, 2003; Viereck-Götte and Gürel, 2003; Le Pennec *et al*., 2005); there is no information available concerning the distribution and origin of clay minerals in either the volcanic or volcano-sedimentary units.

Thus, the objective of the present study is to demonstrate that paleosols and calcrete intercalations in the carbonates, fluvial sediments, diatomaceous clayey sediment and pyroclastic sediments of the CVP are widely distributed in central Anatolia. Furthermore, the sedimentology, mineralogy and origin of smectite-dominated clay minerals in these units are discussed.

MATERIAL AND METHODS

Field work was carried out using existing geological maps of the İncesu and Güzelöz areas modified from the 1:100,000 scale MTA map. To identify the lateral and vertical distributions of clay minerals, four stratigraphic sections within the study area were examined (Figure 1).

Fifty two samples, representative of the various facies of the Upper Bayramhacılı formation, were analyzed with respect to their mineralogical characteristics by polarized-light microscopy (Olympus-BH-2 3M0548 Pol.), X-ray powder diffractometry (XRD) (Siemens D 5000, Diffrac AT V. 3.1), and scanning electron microscopy (SEM) equipped with energy dispersive X-ray microanalysis (SEM-EDX) (Noran, Cam scan, Pioneer TP 250). The XRD analyses were

* E-mail address of corresponding author:
agurel_1999@yahoo.com
DOI: 10.1346/CCMN.2006.0540503

performed using CuKα radiation and a scanning speed of 1º2θ/min. Unoriented mounts of powdered whole-rock samples were scanned to determine the mineralogies of the bulk samples. Samples for clay analysis (<2 μm) were prepared by separation of the clay fraction by sedimentation, followed by centrifugation of the suspension after overnight dispersion in distilled water. The clay particles were dispersed by ultrasonic vibration for about 15 minutes. Four oriented specimens of the <2 μm fraction were prepared from each sample: they were air dried, ethylene glycol solvated at 60ºC for 2 h, and thermally treated at 350ºC and 550ºC for 2 h. Semi-quantitative analyses of rock-forming minerals were obtained using the external standard method of Brindley (1980), whereas the relative abundance of clay mineral fractions was determined using their basal reflections and the mineral intensity factors of Moore and Reynolds (1989). Representative clay-dominated bulk samples were prepared for SEM-EDX analysis by adhering the fresh, broken surface of each rock sample onto an aluminum sample holder and coating with a thin film (350Å) of gold using a Giko ion coater.

Chemical data for 15 representative samples of paleosols, calcretes, carbonates, fluvial sediments, diatomaceous clayey sediments and pyroclastic sediments from the Upper Bayramhacılı formation were acquired by inductively couple plasma-atomic emission spectroscopy (ICP-AES) for major-element analyses at the ACME Analytical Laboratories Ltd (Canada). In these analyses, detection limits ranged from 0.01 to 0.1 wt.% for major elements, and 0.1 to 5 ppm for trace elements.

REGIONAL GEOLOGY AND DEPOSITIONAL ENVIRONMENTS

The long axis of the CVP extends ~300 km in a NE−SW direction. The CVP is, in large part, situated within the Anatolide tectonic belt. The volcanic province developed within a system of complicated tectono-volcanic extensional depressions during the Middle Miocene to late Quaternary time interval (Türkecan *et al.*, 2003). The Neogene deposits exhibit a gentle topography with respect to the basement units. In most places, the Tertiary and Quaternary sediments, such as lacustrine deposits, paleosols, and fluvial sediments, and a thick succession of volcaniclastic materials, discordantly overlie the basement units comprising Paleozoic-Cretaceous metamorphic (schist, marble, metagabbro) and ophiolitic rocks (late Cretaceous rocks, not shown in the geological map) (Schumacher *et al.*, 1990; Toprak, 1996; Türkecan *et al.*, 2003). In the CVP, lacustrine deposits, paleosols, and fluvial sediments are intercalated with some ten ignimbrite levels. Almost every ignimbrite level covers a wide area of several thousand km^2 and they serve as excellent marker horizons for correlating sediment profiles and paleosols. K/Ar age data on the volcaniclastic sediments indicate an age of 11 to 2.7 Ma for the succession (Innocenti *et al.*, 1975). However, most of the lacustrine deposits, paleosols-calcrete and fluvial sediments occur within the 7.6−2.7 Ma interval (Viereck-Götte and Gürel, 2003).

From bottom to top, the volcanic units consist of andesite and basalt of the Hoduldağ and Tekke volcanics, the Cemilköy ignimbrite, the Kızılkaya ignimbrite, the İncesu ignimbrite, and Quaternery basalt (Figure 1).

The Kızılkaya ignimbrite (Lower Pliocene) is a widespread, welded ignimbrite unit characterized by typical columnar jointing exposed along steep valleys and roads cutting into the wide plateau. According to Schumacher *et al.* (1990), the mean K/Ar age of the Kızılkaya ignimbrite is 4.3 Ma. The İncesu ignimbrite begins with a basal vitrophyre beneath a densely welded central zone, and has an upper part characterized by flattened pumice fragments and thermally altered xenoliths. The İncesu ignimbrite also has a distinct geochemistry, with notably lower SiO_2. K/Ar age data on whole-rock samples of this ignimbrite have yielded an age of 2.7±0.1 Ma (Innocenti *et al.*, 1975; Schumacher *et al.*, 1990). In the study area, fluvial conglomerate-sandstone, lacustrine diatomite, clayey diatomite, limestone and paleosols-calcrete (paleosol II and lacustrine carbonate) were deposited between the Kızılkaya and İncesu ignimbrites during the Pliocene.

Lithofacies distribution

The Pliocene Güzelöz-İncesu plateaus are split into southern and northern branches (Figure 1). A large volume of siliceous, siliciclastic and carbonate sediments was deposited in the southern branch, characteristic of lake to very shallow lacustrine environments, whereas the northern branch is characterized by lake-margin and lake sediments, typical of narrow, elongate lake to shallow lacustrine environments (Figure 1). Six lithofacies have been distinguished within the Pliocene sediments of the Güzelöz-İncesu plateaus; these lithofacies are adapted from Miall (1996; Figures 2 and 3).

Massive conglomerates (Gm). Massive, unsorted, rounded-clast, pink conglomerates make up this facies; these conglomerates are mainly matrix-supported and may contain as much as 10% unsorted matrix, and the average clast size is ~5 cm. Measured profiles in this lithofacies range between 1 and 2 m. The paleoflow direction was generally N−S. The presence of lens-shaped layers, normal grading, and oriented clasts indicate river involvement.

Trough cross-bedded sandstone (St). This lithofacies comprises medium- to coarse-grained sands and contains ripples with curved foresets and asymptotic downlap at its base. The thickness of the layers varies between 10 and 30 cm, and the thickness of trough cross-bed sets is ~3 mm. Outcrops of this facies are relatively limited.

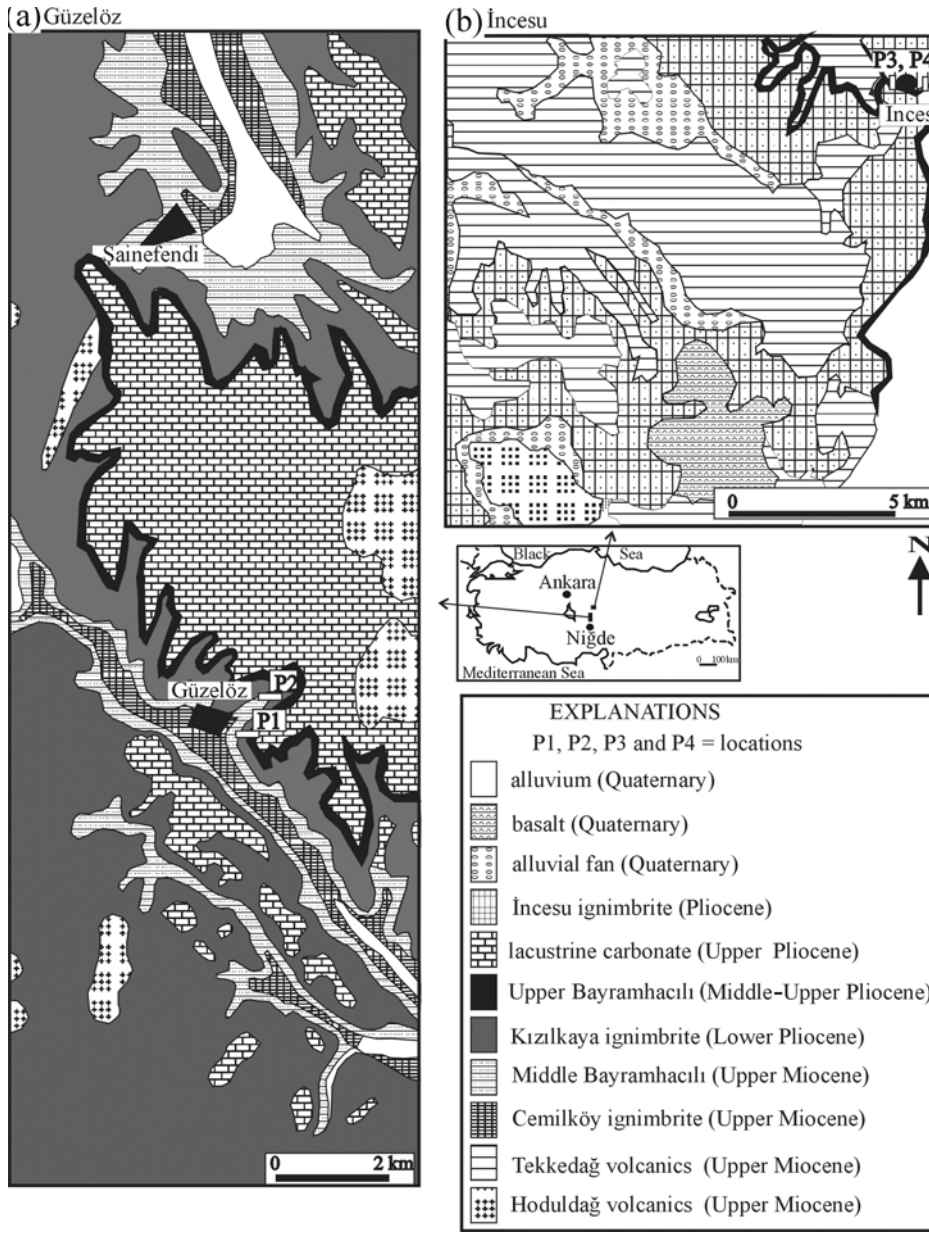

Figure 1. Generalized geological map of the (a) Güzelöz, and (b) İncesu areas (modified from 1:100,000 scale MTA map, 1989).

Paleosol (AL-P). These paleosols, composed of clayey and coarse-grained components, are moderately developed (Retallack, 1988), and locally enclose scattered pumice pebbles, near-surface root zones, and subsurface clayey, sesquioxide-rich areas. The most mature soils are associated with fluvial overbank deposits at some distance from the main channels, which were the source of incremental additions of fine-grained sediments. Overbank deposits proximal to paleochannels have more preserved bedding and less mature paleosols, and pedogenic disruption of bedding and paleosol maturity increase away from channels towards more distal floodplain settings.

Massive calcrete (AL-Ca). Reddish brown, massive calcretes comprise tuff and pumice clasts cemented and replaced by calcite, and grade downwards into calcareous tuff and pumice clasts; these rocks range in thickness from 20 cm to 3 m. The upper part of well developed massive calcrete is hard, well cemented and porous, and grades downwards through softer calcrete and paleosol into quite porous calcareous tuff and pumice clasts. Consequently, the massive calcrete is typically characterized by non-uniform cementation which accentuates surface cavities. Both paleosol and calcrete lithofacies of the İncesu and Güzelöz districts are dominated by smectite, lesser amounts of illite, and local traces of kaolinite.

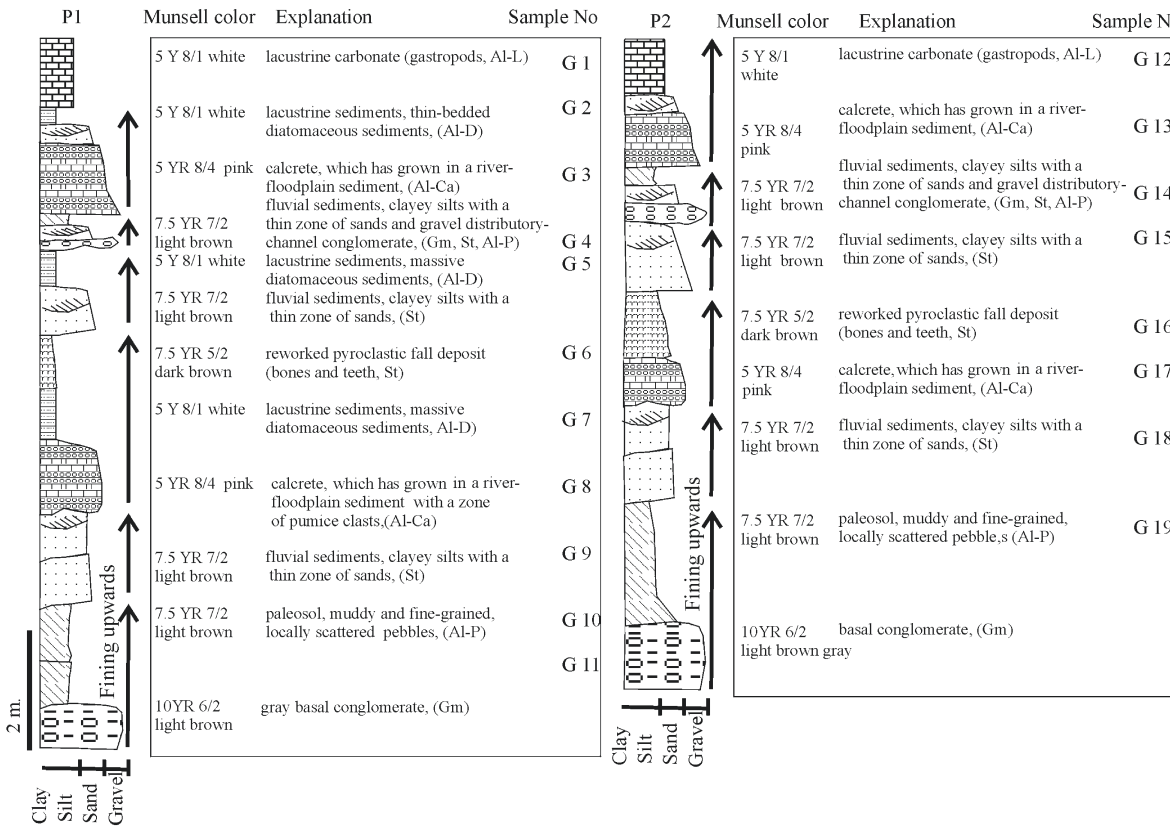

Figure 2. Distribution of the principal lithologies of the Güzelöz (P1, P2) areas (see Figure 1 for section locations and Table 1 for mineralogical compositions of the samples).

Limestone (AL-L). Micritic limestone beds with diatomite intercalations make up this facies. Locally the limestone is brecciated and contains abundant microcavities. Biogenic components are mainly fragments of fresh-water molluscs, but plant remnants are also present sporadically.

Diatomite (AL-D). The lower–middle parts of profiles P1, P2 and P3 from the Güzelöz-İncesu plateaus are usually a white, massive clayey diatomite or laminated diatomite, which overlie either paleosols or trough cross-bedded sandstone of overbank deposits.

Description of the stratigraphic sections

Güzelöz area (southern branch). Two sections have been studied near the village of Güzelöz. The first (Figure 2, P1) is located at the northern entry to the village, on the right side of the Güzelöz-Ürgüp road. Section P1 begins with basal conglomerates. It consists of intraformational conglomerates with reworked sesquioxide and pumice clasts, deposited over the Kızılkaya ignimbrite, thus retarding the first stage of lake formation. This conglomerate horizon is overlain by the paleosols (2 m, Al-P). Each paleosol is composed of muddy and fine-grained locally scattered pebbles. They are overlain by overbank deposits, which include silty, trough cross-bedded sandstones (1.5 m, St). These are overlain by the first calcrete of section P1 (1 m). Calcretes, which have grown in a river floodplain sediment with a zone of pumice clasts, have significant volume in the Güzelöz profile (Figure 2, Al-Ca). These units overlie lacustrine sediments, namely massive diatomite, reworked pyroclastic-fall deposits containing bones and teeth, and clayey silts with thin sandbank partings (Al-D, St, Al-D). The next overbank cycle begins with bedded and polymictic conglomerates which were redeposited by fluvial processes and consist of volcanoclastic and magmatic rock clasts, trough cross-bedded sandstones, which are often interbedded with moderately developed paleosol (Retallack, 1988), and calcrete at the top of the preceding cycle (Gm, St, Al-P and Al-Ca). This calcrete (1.5 m) is second of section P1 and it is grown in river floodplain sediments. This horizon is overlain by a trough cross-bedded sandstone, and massive diatomite. Lacustrine carbonates sit on this section.

The second section (Figure 2, P2) is located ~600 m south along the access to the motorway where the lower layers of paleosols are better exposed. This section does not consist of diatomite horizons and other peculiarities of the section P2 are similar to those of section P1. This indicates that the diatomite was deposited as lens bodies in small ponds.

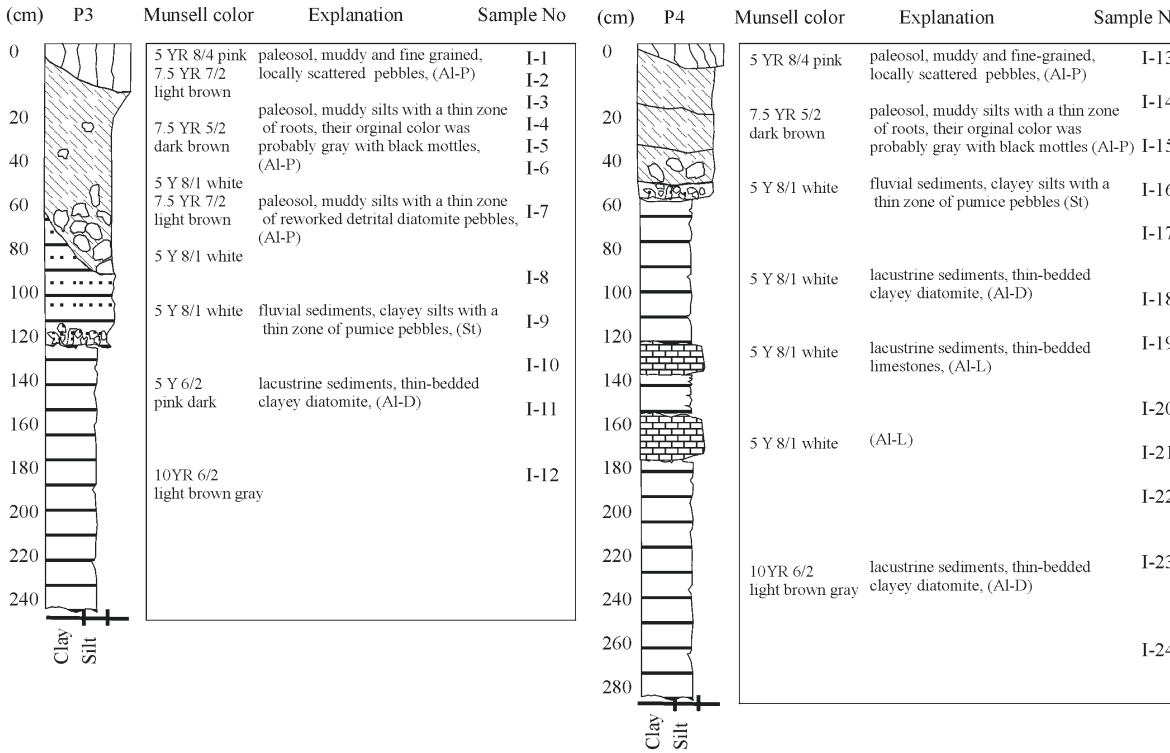

Figure 3. Distribution of the principal lithologies of the İncesu (P3, P4) area (see Figure 1 for section locations and Table 2 for mineralogical compositions of the samples).

İncesu area (northern branch). Two sections have been studied near the town of İncesu. The first (P3) is located at the eastern entry of the town, on the south side of the İncesu–Ürgüp road. Section P3 (Figure 3) begins with thin-bedded clayey diatomite (1.2 m, Al-D). They are overlain by overbank deposits (0.45 m, St), which include clayey silts, and sands with a thin zone of pumice pebbles. A paleosol horizon occurs at the top of the section P3. It consists of three dominant paleosols: (1) a Histosol, with a surface organic horizon of carbonaceous peat and a precompaction thickness of 30 cm; (2) an Aridisol, muddy and fine-grained, with locally scattered pebbles and light coloration (pink), as well as a thin calcareous layer near the surface of the horizon; (3) an Alfisol, with a well differentiated (B, C horizons) profile, of which the subsurface B horizon is appreciably enriched in clay and sesquioxides.

The second section (Figure 3, P4) is located ~200 m west along the access to the motorway where Histosols are better developed. Section P4 does not contain thin-bedded limestones; the other characteristics of this section resemble those of section P3. The total thickness of sections P3 and P4 is ~3 m, but the discordant basal contact with the Kızılkaya ignimbrite is not seen anywhere in the İncesu area. However, this contact is observed in the neighboring Güzelöz area and from the evidence of these outcrops it is likely that a few tens of meters from the lower parts of sections P3 and P4 are missing from the sequence in the İncesu area.

Geomorphology of the Güzelöz area

The Güzelöz ignimbrite plateaus are at 1580–1600 m in altitude corresponding to Upper Miocene denudation surfaces (Figure 4, D II, Erol, 1999). Tectonically controlled basin subsidence occurring within the Sultan basin at the beginning of the Pliocene resulted in depression of the basin's base level. Denudation and fluvial erosion processes governed by Pliocene temperate and semi-humid climate conditions and a depressed base level prevailed in the study area. Subsequently, gently inclined erosional surfaces emerged. They are locally merged into the denudation surfaces of the Upper Miocene as fluvial troughs following weak tectonic and lithological paths. The study area includes one of these fluvial troughs. Pliocene erosion surfaces are at ~1520–1580 m and consist of thick ridges such as Lalebeni Sırtı, Yelekbaşı Sırtı, Kanlılovak Sırtı, and Büyük Çakıl Tepe Sırtı (Figure 4, D III, Erol, 1999). Upward, these surfaces cut Upper Miocene denudation surfaces and contain minor closed basins where ponds and/or small lakes were developed under suitable climate conditions.

The young Güzelöz-Yeşilhisar valley is developed at the base of a Pliocene erosional trough as a result of base level depression of the Sultan basin. Glacis-type terraces ~50–80 m in height from the base of the valley were developed in the further parts of the valley. Sheet floods and sheet erosion developed under early Pleistocene continental-subtropical climate conditions. Consequently,

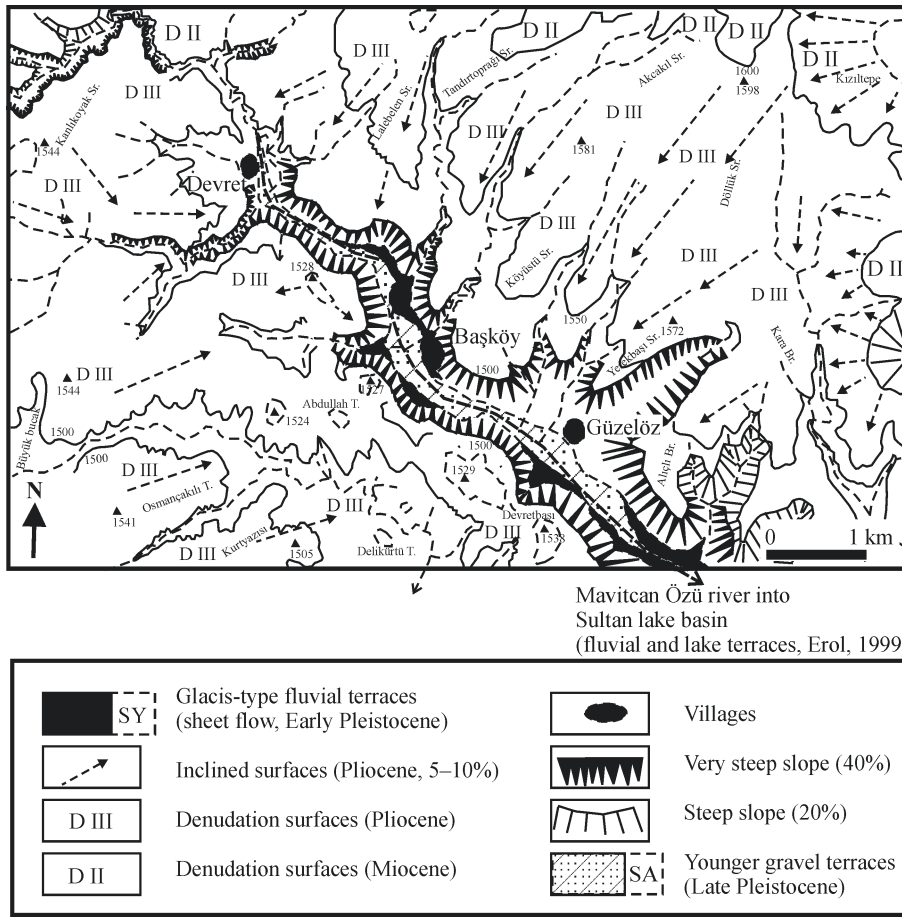

Figure 4. Geomorphological map of the Güzelöz area.

slopes of the area were eroded resulting in the development of glacis-type fluvial terraces (Figure 4, SY, Erol, 1999). Young gravel terraces of late Pleistocene age were developed valleyward (Figure 4, SA, Erol, 1999). These terraces occurring in two levels, 10 and 30 m, were caused by the final depression of the base of the valley during the late Pleistocene.

RESULTS

Petrography

The pyroclastic units of the area are composed of isotropic amorphous materials of volcanic units, in addition to irregular volcanic glass-shard particles, clinopyroxene (diopside), rarely orthopyroxene (hypersthene), plagioclase (mainly oligoclase, rarely labradorite and bytownite) and rare K-feldspar (sanidine) phenocrysts of the ash-flow tuff (Figure 5a–e). Glass-shard particles are generally rimmed by alteration products, whereas pyroxene crystals are highly altered and chloritized, plagioclase and K-feldspar are partially to completely altered. The matrix between these particles and minerals consists of volcanic materials and alteration products. Thin-sections from paleosol and calcrete samples show irregular clay nodules cemented by microsparitic to sparitic meniscus cement similar to that reported by Hay and Reeder (1978), Riding and Wright (1981), Wright (1983, 1986, 1987) and Karakaş and Kadir (1998) (Figures 5f). Also, some of the fractures, desiccation cracks and geopetal-type fenestrae are filled with dogtooth-type sparitic crystals similar to those reported by Siesser (1973), Warren (1982a, 1982b) and Kadir *et al.* (2002) (Figure 5g). Both XRD and EDX analyses reveal that the microsparitic and sparitic crystals – both fill and cements – are composed of calcite.

XRD determinations

The XRD results for bulk samples from several profiles in both the Güzelöz and İncesu regions are given in Tables 1 and 2. Smectite and illite are the predominant clay minerals, locally associated with accessory kaolinite and sepiolite. Smectite predominates mainly in the paleosol, calcrete, diatomaceous sediment samples, and less so in fluvial sediments of the İncesu and Güzelöz districts. These clay minerals are accompanied by mainly plagioclase, K-feldspar, quartz, calcite, opal-CT, pyroxene (petrographically determined as diopside and rarely hypersthene) and, locally, traces of gypsum.

Table 1. Mineralogical variation through the stratigraphic sections of the Güzelöz areas (see Figures 1 and 2 for sample locations).

	Rock type	smc	ill	kao	sep	fds	px	cal	gyp	qtz	op
In*						+++++	++++				acc
G 1	Carbonate		+					+++++	acc	acc	
G 2	Clayey dia lac sd	++	+	acc		+++	acc	++		++	+
G 3	Calcrete	+++	acc			++		++		+	+
G 4	Fluvial sed	++	+	+		+++	+	+		++	+
G 5	Clayey dia lac sd	++	+			acc		++++		+	
G 6	Pyroclastics	++	+	acc	acc	++++		+		++	
G 7	Clayey dia lac sd	+++	+	acc		++		++		++	+
G 8	Calcrete	acc	+			+		+++		+	+
G 9	Fluvial sed		++	+		+++	+			++++	+
G 10	Paleosol	++++	+			+++++	+			++	acc
G 11	Paleosol	+++	+			++++	+			++	acc
G 12	Carbonate							+++++		acc	
G 13	Calcrete		+			+		+++++		+	acc
G 14	Fluvial sed		+	acc		+++				++++	acc
G 15	Fluvial sed		+	acc		+++				++++	acc
G 16	Pyroclastics	+++	+	acc	acc	++++		++++		+	
G 17	Clacrete	++	+			+++		+++++		++	+
G 18	Fluvial sed		+++	+		++	+			++++	acc
G 19	Paleosol	+++	+			++++	+			++	acc
K†			+++			+++++	acc			++	

smc: smectite, ill: illite, kao: kaolinite, sep: sepiolite, fds: feldspar, px: pyroxene, cal: calcite, gyp: gypsum, qtz: quartz, op: opal-CT, Fluvial sed: fluvial sediment, Clayey dia lac sd: clayey diatomaceous lacustrine sediment +: relative abundance of mineral phase, acc: accessory, *In: İncesu ignimbrite, †K: Kızılkaya ignimbrite.
Data sources: Temel *et al.* (1998), Toprak *et al.* (1994), Le Pennec *et al.* (1994), L. Viereck-Goette (pers. comm., 2004)

Table 2. Mineralogical variation through the stratigraphic sections of the İncesu areas (see Figures 1 and 3 for sample locations).

	Rock type	smc	ill	kao	sep	fds	px	cal	gyp	qtz	op
In*						+++++	++++				acc
I-1	Paleosol	++++	+			+++	acc	acc	acc	++	+
I-2	Paleosol	++++	+			++				+	+
I-3	Paleosol	+++++	+			++++			acc	+	+
I-4	Paleosol	+++++	+			++	++			+++	+
I-5	Paleosol	+++++		acc		++	+			+++	+
I-6	Paleosol	+++++	++	+		++				+++	acc
I-7	Paleosol	++	+	+		+++	+			+ +++	acc
I-8	Fluvial sed	+	++	acc		+++	++			++++	+
I-9	Fluvial sed		+			++++	++			++	++
I-10	Clayey dia lac sd	++	+			+++				+	++
I-11	Clayey dia lac sd	+++	acc			++++	acc			++	+
I-12	Clayey dia lac sd	++++				++++	acc			++	++
I-13	Paleosol	+++	+			+++++	acc	+		++++	
I-14	Paleosol	++++	+		acc	++++	+			+	+
I-15	Paleosol	+++	++		acc	++++	+			++	+
I-16	Fluvial sed	++	+			+++	acc			+++	+
I-17	Fluvial sed	++++				++++				++	++
I-18	Clayey dia lac sd	++	+			+++	acc			+++	+
I-19	Carbonate	acc						+++++		acc	
I-20	Clayey dia lac sd	++	+			++++				++	+
I-21	Carbonate							+++++		acc	
I-22	Clayey dia lac sd	+++	+			++++				++	++
I-23	Clayey dia lac sd	++++	acc			++++				+	++
I-24	Clayey dia lac sd	++	+			+++				++	+
K†			+++			+++++	acc			++	

* Abbreviation and sources as in Table 1.

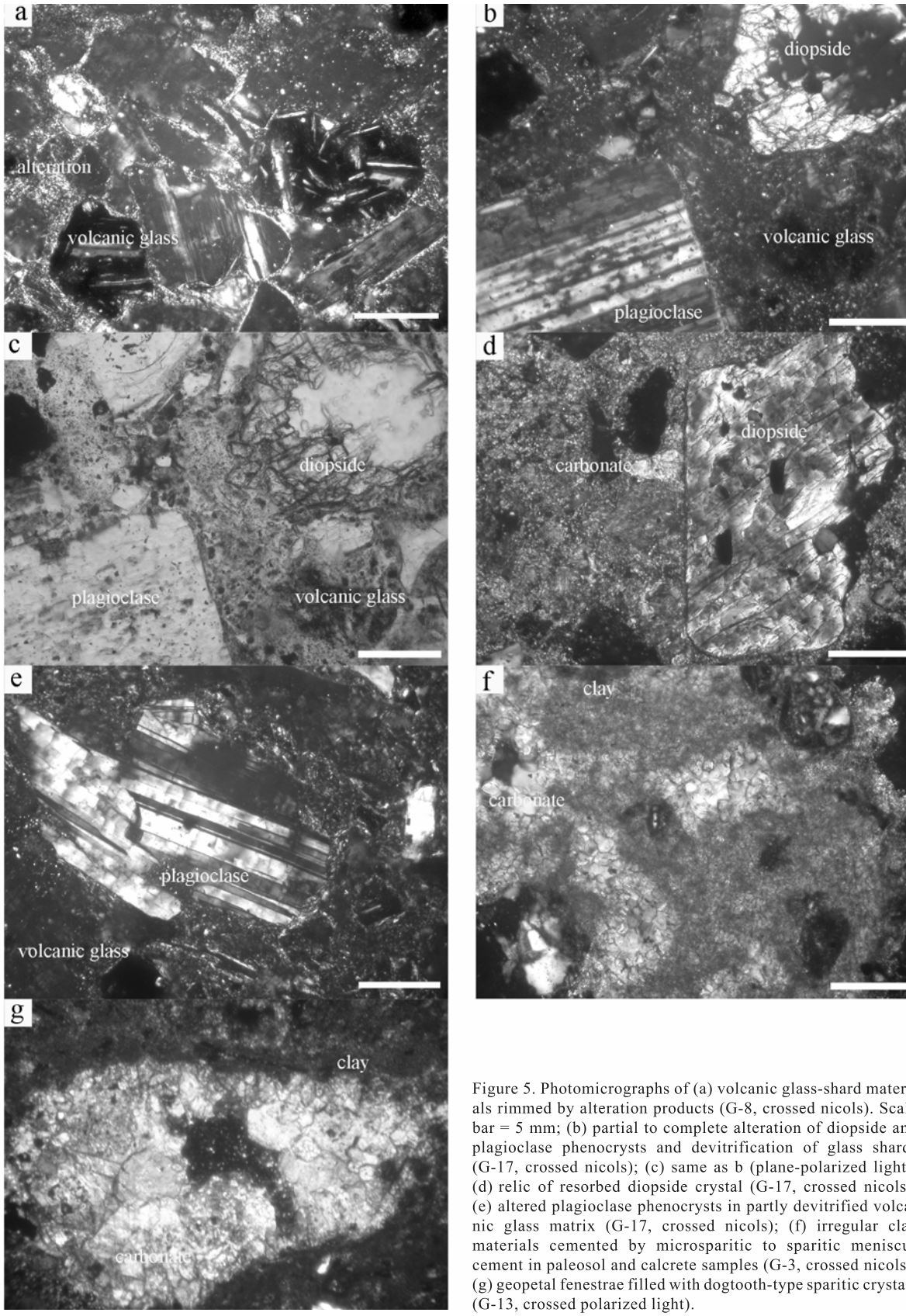

Figure 5. Photomicrographs of (a) volcanic glass-shard materials rimmed by alteration products (G-8, crossed nicols). Scale bar = 5 mm; (b) partial to complete alteration of diopside and plagioclase phenocrysts and devitrification of glass shards (G-17, crossed nicols); (c) same as b (plane-polarized light); (d) relic of resorbed diopside crystal (G-17, crossed nicols); (e) altered plagioclase phenocrysts in partly devitrified volcanic glass matrix (G-17, crossed nicols); (f) irregular clay materials cemented by microsparitic to sparitic meniscus cement in paleosol and calcrete samples (G-3, crossed nicols); (g) geopetal fenestrae filled with dogtooth-type sparitic crystals (G-13, crossed polarized light).

Plagioclase and quartz are dominant in most of the samples, whereas calcite is abundant in several levels in the Güzelöz profile and in samples I-1, I-19 and I-21 of the İncesu area. There is an inverse relationship between opal-CT and calcite. Therefore, the proportion of opal-CT is relatively high in the diatom-bearing İncesu section where calcite is generally absent (except in some levels), and low in the Güzelöz section where calcite is abundant.

The smectite is characterized by reflections at 14.5–15.8 Å (Figure 6). These peaks expanded to 16.7–17.3 Å following ethylene glycol solvation, and collapsed to 9.82 Å upon heating to 350ºC; additional heating to 550ºC caused further reduction in sharpness and reflection of the peaks. The d_{061} reflection varied from 1.49 to 1.50 Å, possibly indicating the occurrence of dioctahedral smectite (Moore and Reynolds, 1989). The illite is indicated by reflections at 10 and 5 Å, and kaolinite by 7.16 and 3.57 Å peaks. The basal reflection of kaolinite at 7.16 Å collapsed upon heating to 550ºC. Sepiolite is characterized by 12.35 Å and gypsum by 7.60 Å peaks. An increase in the XRD background in most of the samples may indicate the presence of opal-CT (Jones and Segnit, 1971; Iijima, 1980; Iijima and Tada, 1981) as well as biogenic materials (such as diatoms in the İncesu-area samples), similar to those reported elsewhere (Henderson *et al.*, 1971; Kastner, 1979; Stamatakis *et al.*, 1989).

Scanning electron microscopy

Güzelöz area. In the paleosols of the Güzelöz profiles, authigenic K-feldspar occurs either as euhedral or subhedral blocks (with dimensions of 12 μm × 60 μm × 30 μm) in dissolution voids and vugs (Figure 7a). These crystals are surrounded by lepispheres composed of sub-rounded accumulations of acicular crystals (1 μm) of opal-CT (Figure 7b). Some of the feldspar crystals are partially to highly resorbed, resulting in oriented, irregular, bar-shaped remnants of feldspar grains (Figure 7c). Although the morphology of these grains is not diagnostic, identification thereof was based on XRD analyses of the bulk samples and EDX analyses of the remnants.

Some glass-shard relics in the paleosol exhibit dissolution voids (Figure 7d); the diameters of these voids are ~5–25 μm. Locally, the edges of these voids are partially coated by mainly authigenic smectite. Relics of bar-shaped, irregular grains are coated by spongy-textured material, apparently reflecting smectite (Figure 7e). The altered feldspar and glass-shard relics are mainly cemented by spongiform clays. The feldspar crystals have sub-rounded outlines and hollow centers, both of which resulted from dissolution processes.

Bar-shaped, platy, and sub-rounded forms characterize relict feldspar and accessory glass shards, both of which are cemented, coated and covered by spongy material, possibly reflecting smectite. In sample P3, wavy flakes and spongy structures on feldspars and glass shards are smectite, which in turn locally overgrow fibrous materials which resemble illite.

In the calcrete, euhedral authigenic rhombic calcite crystals (60 μm in diameter) occur abundantly, and are partially altered or dissolved (Figure 7f).

In the fluvial sedimentary units, relatively large, irregular detrital feldspar crystals are cemented by a fine, detrital quartz matrix (Figure 7g). The feldspar exhibits vesicular-type degradation and irregular outlines (Figure 7h). Some of the vesicles in feldspar enclose authigenic euhedral crystals of a neoformed mineral – possibly aragonite or calcite – insofar as degradation of feldspar may result in the removal of Na and relative enrichment of Ca due to differences in their mobilities. Also, authigenic euhedral feldspar is developed in vugs and dissolution voids of fine detrital quartz. The degradation process in feldspar as well as in detrital quartz is an important source of Si for the development of authigenic euhedral quartz and alteration products (Figure 7i).

Moreover, traces of accordion-like kaolinite – exhibiting face-to-face stacks of pseudohexagonal plates of books – also occur locally; these features are only slightly degraded (Figure 7j).

İncesu area. In the lacustrine clayey-diatomaceous sedimentary units, relatively large blocky feldspar grains (with dimensions of 10–40 μm × 7–10 μm in diameter) are partially to highly dissolved. Also, this unit is dominated by bar-shaped, ellipsoidal- and fan-like structures that have sieve, honeycomb or cellular textures of diatoms. The diatom-bearing sediments are cemented mainly by a flaky alteration product, either smectite or smectite-illite-type clay minerals. Some of these structures are unaltered; only a few are partially degraded, due to sedimentary processes, local tectonic activity, or both.

Also, devitrification of glass-shard relics and dissolution of feldspar have been observed, and alteration products – such as smectite – are the main cements in these units (Figure 7k).

The EDX analysis has shown that the spongiform clay that resembles smectite is composed mainly of Si, smaller amounts of Al, and lesser Fe, Mg and Ca (Figure 8a). Feldspar crystals are characterized by a strong peak for Si, followed by a smaller peak for Al and very faint peaks for Mg, K, Ca and Fe (Figure 8b). Furthermore, the altered volcanic rocks with rounded dissolution voids are also composed mainly of Si, with very small peaks for Al, followed by those for Mg, K, Ca and Na (Figure 8c). Decreasing Si and increasing Al, related to altered feldspar and volcanic glass, contributed to the development of spongy smectite, indicating that both feldspar and glass shards were important sources of Si, Al, Mg and Fe, similar to the situation reported by Kadir and Karakaş (2002) and Kadir *et al.* (2002).

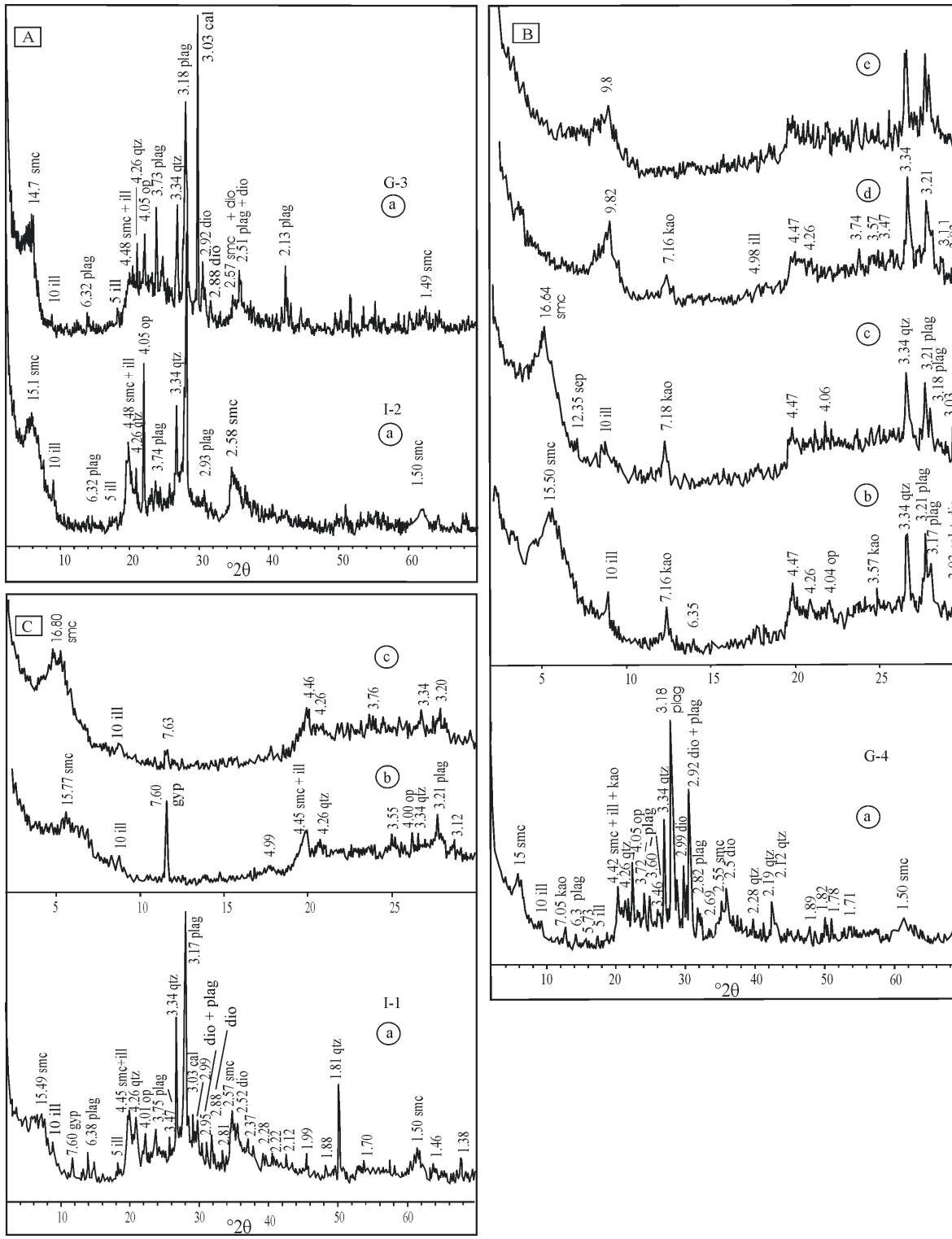

Figure 6. XRD patterns for the smectite-dominated materials: (A) G-3, I-2; (B) I-1 and (C) G-4 samples. smc: smectite, ill: illite, kao: kaolinite, sep: sepiolite, plag: plagioclase, dio: diopside, qtz: quartz, op: opal-CT, cal: calcite, gyp: gypsum (a = powder, b = oriented, c = ethylene glycol solvated, d = heated to 350ºC, e = heated to 550ºC treatment). Spacings in Å.

Chemical analyses

Representative chemical analyses of paleosol, calcrete, fluvial sediments, diatomaceous clayey sediments, carbonate and pyroclastic samples are given in Table 3. The representative paleosol samples are characterized by high Al_2O_3, Fe_2O_3 and SiO_2; these values reflect feldspar and a large smectite (montmorillonite) content in the samples. The linear relationship between Al_2O_3 and Fe_2O_3 indicates that these oxides are present mainly in smectite on the basis of mineralogical determinations. The Al_2O_3 contents increase with an increase in clay or SiO_2. A high SiO_2 content in the whole-rock analyses is attributed to the presence of quartz, feldspar, opal-CT and diatoms, as well as clay minerals (Tables 1, 2, 3). However, SiO_2 contents are enriched in the paleosols, fluvial and diatomaceous clayey sediments in contrast to the SiO_2 values for carbonate and calcrete samples. The CaO content is attributed mainly to calcites, which has a sub-parallel relationship with loss on ignition, and occur mainly in the interlayer space of smectite. The clay content decreases with increase in $CaCO_3$. The non-carbonate fraction is, therefore, quite rich in aluminosilicate minerals. Thus, the presence of an inverse relationship between CaO and other oxides may correspond to an inverse relationship between calcite and other minerals. The MgO content seems to be directly related to mainly volcanic materials such as diopside and hypersthene. The pyroclastic sample (G-6) also contains large amounts of SiO_2, Al_2O_3 and Fe_2O_3 and small amounts of CaO and MgO. The K_2O in the samples is attributed to the presence of some K-feldspar and illite.

Trace elements such as Zr, Ba, Cr, Cu and Zn are immobile and are enriched in paleosol levels. Co, Ni, Pb, Nb, V and Y are generally constant and unaffected by alteration processes, whereas Sr decreases slightly with a depletion of Ca, and Th increases slightly in most of the altered samples relative to the pyroclastic rocks. Therefore losses and gains of elements in the profiles are controlled by the alteration process, mobilities of elements, and porosities.

DISCUSSION

Evolution of the Güzelöz-İncesu plateaus

The region investigated in this paper is located in the Güzelöz-İncesu plateaus, which are ~60 km across, within the CVP. NNE−SSW and E−W oriented faults have been reported around the Güzelöz-İncesu plateaus (Türkecan *et al.*, 2003). Evolution of the plateaus commenced following the diminution or complete cessation of volcanic activity around the Güzelöz-İncesu plateaus (in particular, the Kızılkaya ignimbrite). When the lacustrine system had completely developed, two distinct paleogeographic domains with individual characteristics resulted (very shallow lacustrine stage in the southern branch and shallow lacustrine stage in the northern branch, Figures 2, 3, 4).

Very shallow lacustrine stage (southern branch). Based on observations of the fluvial terraces, the Güzelöz plateau was from time to time connected to the Sultansazlığı lake by rivers which traversed its northern part during the Pliocene (Figure 4). Therefore, the geological and geomorphological history of the Güzelöz plateau is tied closely to its northern part. Today, the plateau is open to outward drainage by the Mavitcan Özü river and its tributaries. At the end of the Pliocene, the fluvial course of the Mavitcan Özü river was deflected to the south of Güzelöz by tectonic activities and, consequently, a narrow, extended lake fed by a lateral and longitudinal drainage system developed in Güzelöz. That river flows N−S and discharges into the southern end of a very narrow, shallow lake. The basin filled with several meters of clastic sediments during the Pliocene, following formation of a very shallow lake, and deposition occurred in a variety of lacustrine and fluvial environments. The components of this mosaic lack a consistent lateral relationship to the major channel deposits. That is, dry and wet areas were not predictably near or far from the active channels. The thickness of an overbank sequence at any given site was controlled by topographic lows in the floodplain and by the level above which sediment could no longer accumulate, the point where avulsion shifted deposition to another area. In the measured section we identified six fining-upwards sequences, which are indicative of fluctuation of water levels in the area. Rainy conditions in central Anatolia would have caused seasonal fluctuation in the water table of the Güzelöz-İncesu plateaus and intense evapotranspiration in the sedimentary basin during the dry season. The disrupted internal fabric and highly variable vertical distributions of sesquioxide and $CaCO_3$ in the massive calcrete (AL-Ca) suggest that weak bioturbation may have been more responsible for preventing the formation of clear paleosols than in the leached zone and overlying concentrations of limestone (Figure 2). Lateral texture variation in the limestone suggests that carbonate accumulation was controlled by local drainage conditions. Calcrete is found mainly in semi-arid parts of the Mediterranean region, though Wright (1982) has described calcrete from some sub-humid and subtropical areas of the world. This generally accepted paleoenvironmental model for calcrete formation was repeated during arid-humid climatic fluctuations in the Pliocene.

Shallow lacustrine stage (northern branch). The type of clayey material discharge related to lateral drainage depends also upon the structural framework. Massive and layered diatomites were deposited in the small ponds fed by overflowing, very shallow lakes, and to a lesser extent, by lateral drainage during the Pliocene. During rainy seasons, clayey diatomites were also deposited. Temperature increase would have contributed to calcite saturation (limestone, Figure 3, P4). In this section there was no fluvial input compared with section P3. For that

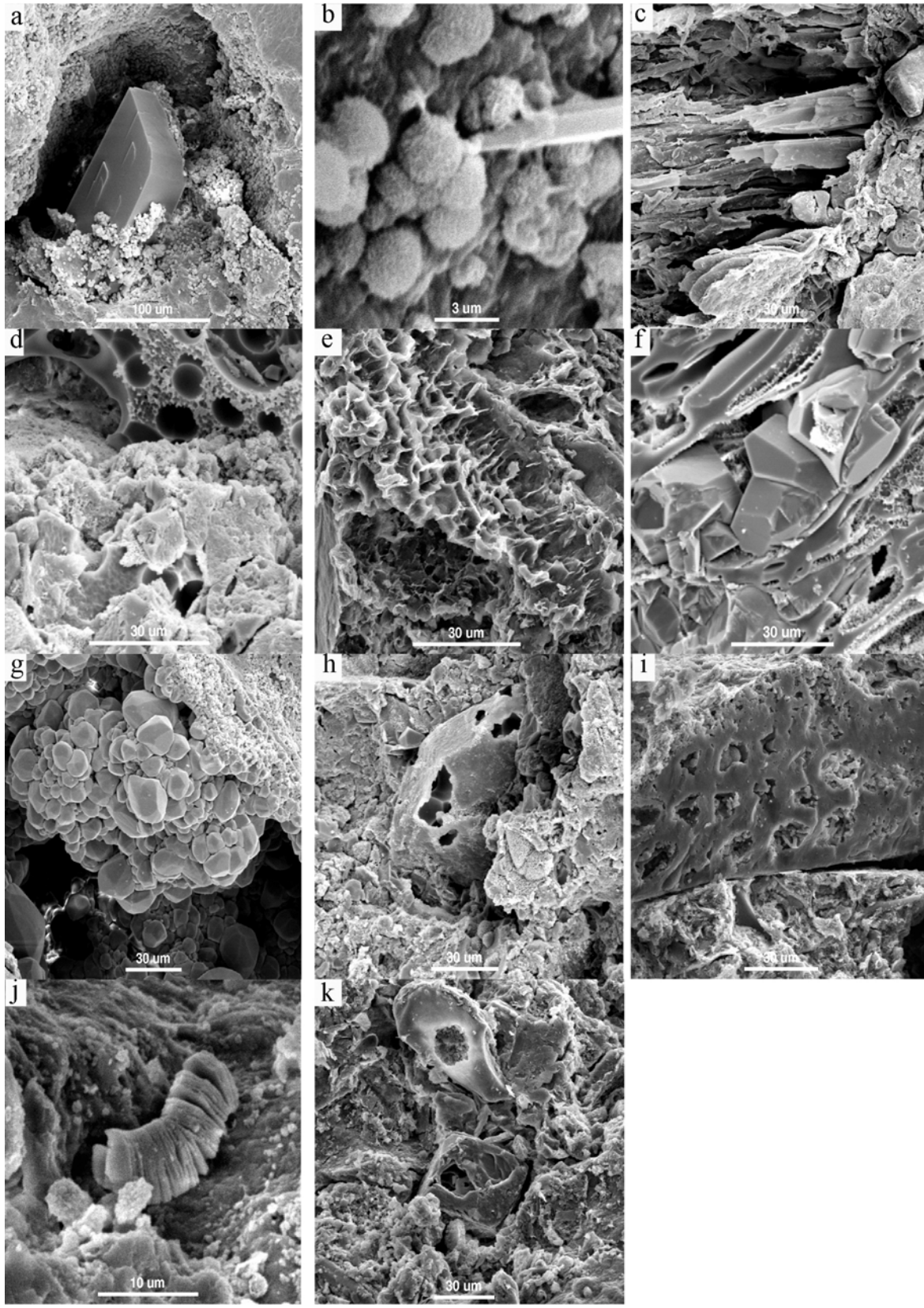
a
100 um
b
3 um
c
30 um
d
30 um
e
30 um
f
30 um
g
30 um
h
30 um
i
30 um
j
10 um
k
30 um

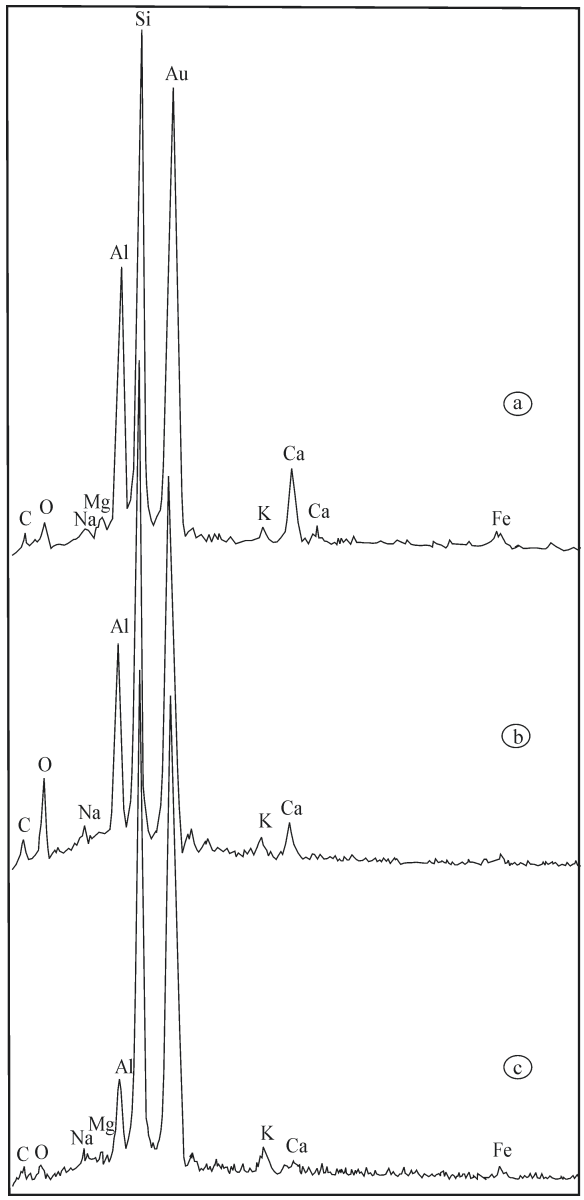

Figure 8. EDX analysis of (a) smectite (I-14), (b) feldspar (G 3) crystals, and (c) glass shard (G 3).

reason, the water conditions were suitable for $CaCO_3$ concentration. According to Schreiber and Tabakh (2000), carbonates form under evaporative conditions in ponds having salinities of 120–150 g/L and are commonly similar in appearance to non-evaporative pond deposits. The major difference is that there are few or no fossils and little or no burrowing in evaporative sediments. Live diatoms persist up to salinities of 36–80 g/L (pelletal mud, intercalated diatomite) and 80–140 g/L (carbonate, diatomite, gypsum), but with a very restricted population of only two species by 128 g/L (Noel, 1984). Based on lithofacies features of the diatomite-limestone in the İncesu area, it is concluded that, during the late Pliocene, hot and humid seasonal wet-dry climates reached a maximum, but that the effects of vegetation (in building paleosols and relative to erosional processes) reached a minimum. The lake that developed in the northern branch was significantly shallower during the late Pliocene, and climate changes resulted in the development of the Upper Bayramhacılı formation in permanent (or seasonal) swamps and lakes and on topographically higher, drier land surfaces where paleosols were formed. The succession consists of three dominant paleosols: (1) a Histosol; (2) an Aridisol; and (3) an Alfisol.

Widespread diatomite, limestone and paleosol-calcrete were deposited in the shallow lakes of central Anatolia and particularly in the CVP. The presence of diatomite-limestone deposits in the Hırka-Kızılırmak basin was reported previously by Uygun (1976), whose study reported the presence of diatomite deposited in the CVP during the Pliocene. Subsequently, diatomite and limestone deposits in Nevşehir-Ürgüp-Ihlara-Selime areas adjacent to the Güzelöz-İncesu plateaus were discovered (Gabriel and Malecha, 1972), and these stratigraphic horizons may even be considered as ideal marker beds, in addition to the ignimbrites.

Origin of clay minerals

Following regression of the sea from central Anatolia, several lacustrine paleo-environments developed. Diatom-bearing sedimentary and volcano-sedimentary units, such as mudstone, limestone and reworked pyroclastic rocks, began to be deposited. Upwards from the stratigraphic levels where paleosol and calcrete are abundant, diatoms disappeared due to tectonic and climatic (arid and semi-arid) changes, similar to those reported by Galán and Ferrero (1982) and Stamatakis *et al.* (1989). Also, the presence of mottling, sesquioxide, root traces, rhizoids and burrows in continuous, fine-bedded and laminated beds of paleosol, calcrete, and the occurrence of bone- and teeth-bearing reworked pyroclastic materials in the study area, indicate a shallow environment (Wright and Tucker, 1991). These environments are dominated by

Figure 7 (*facing page*). SEM images of (a) authigenic euhedral blocky feldspar crystal in dissolution void (G 3); (b) lepisphere or acicular crystals of opal-CT (G 3); (c) oriented irregular, bar-shaped feldspar relics (G 3); (d) remnants of glass shards in paleosol characterized by sieve texture, and (e) partially coated by spongiform clays (I-14); (e) altered feldspar and glass-shard relics mainly cemented by spongiform clays (G 8); (f) euhedral, authigenic rhombic calcite in partially dissolved feldspar (G 17); (g) fine-grained detrital quartz matrix cementing detrital feldspar crystals (G 13); (h) partially degraded feldspar enclosing authigenic euhedral crystals of aragonite or calcite in its vesicle (G 14); (i) dissolution voids of feldspar and development of alteration products (G 15); (j) accordion-like pseudohexagonal kaolinite (I-4); (k) devitrification of volcanic-glass shards (G 3).

Table 3. Chemical compositions of various lithologies of the study area (see Figures 2 and 3 for sample locations, and Tables 1 and 2 for mineralogical compositions of the samples).

Wt.%	I-1* paleo	I-2* paleo	I-3 paleo	I-7 paleo	G-11 paleo	G-3 calcr	G-8 calcr	G-4 fluv	I-9 fluv	I-12* diat s	G-2 diat s	G-7 diat s	I-19 carb	G-1 carb	G-6 pyroc
SiO_2	55.38	57.42	71.43	61.38	58.12	20.01	22.55	65.20	64.24	55.56	53.90	60.50	5.64	9.00	56.42
TiO_2	0.70	0.70	0.43	0.63	0.76	0.17	0.02	0.58	0.60	0.78	0.03	0.03	0.06	0.02	0.67
Al_2O_3	14.41	16.10	8.76	13.50	14.69	5.04	5.12	8.20	13.85	15.09	8.01	9.01	1.45	1.20	15.25
ΣFe_2O_3	6.36	6.80	5.92	8.84	5.73	1.39	1.42	2.40	5.53	6.47	1.98	0.95	0.69	0.70	9.20
MnO	0.11	0.07	0.04	0.07	0.10	0.06	0.07	0.06	0.03	0.06	0.19	0.20	0.16	0.12	0.07
MgO	7.30	4.84	2.42	3.42	6.78	1.75	1.29	2.01	3.34	4.88	1.94	1.54	4.86	4.02	3.61
CaO	2.63	1.80	1.37	2.28	2.90	38.02	35.53	5.04	2.65	2.10	13.07	12.09	45.61	47.00	3.47
Na_2O	2.17	2.20	2.30	2.46	1.80	0.01	0.58	0.58	2.55	3.71	0.09	0.09	0.08	0.03	2.91
K_2O	2.21	2.18	1.45	2.36	1.95	2.50	1.19	2.10	1.82	2.38	0.10	0.10	0.15	0.15	2.95
P_2O_5	0.20	0.14	0.26	0.15	0.10	0.04	0.10	0.10	0.45	0.20	0.03	0.03	0.05	0.01	0.30
LOI	8.15	7.34	5.25	5.26	7.02	31.00	31.60	13.68	5.06	7.04	20.55	15.44	41.2	37.74	5.15
Total	99.62	99.59	99.63	100.35	99.95	99.99	99.47	99.95	100.12	98.27	99.89	99.98	99.95	99.99	100.0
ppm															
As	9	10	10	9	32	11	10	8	18	12	21	14	8	14	12
Ba	531	471	292	282	217	309	37	32	402	189	129	138	270	530	523
Cl	2660	1841	6727	3790	5196	11378	1118	120	1580	2025	110	1580	1443	1554	2600
Co	45	122	10	12	15	22	12	15	41	79	48	49	47	14	44
Cr	128	119	55	61	89	139	41	35	49	47	43	56	61	57	150
Cu	104	85	38	56	71	127	18	19	29	35	20	23	28	17	103
Nb	15	19	7	7	9	17	9	9	12	11	14	11	10	9	18
Ni	61	70	26	38	35	63	70	75	29	73	75	84	89	23	64
Pb	21	23	11	16	12	21	22	29	16	27	23	32	17	19	24
Rb	120	121	102	170	111	140	18	24	96	118	113	174	29	30	123
S	412	803	1446	999	1072	3056	65	69	312	346	318	112	314	359	415
Sr	435	420	215	330	293	263	402	520	395	513	538	550	418	195	438
Th	16	20	7	8	8	12	9	12	14	17	10	9	13	14	19
V	91	92	75	300	111	103	121	130	95	115	125	125	120	130	94
Y	40	31	16	17	39	36	18	12	35	32	14	25	21	12	43
Zn	38	158	64	82	134	202	75	79	165	121	150	78	77	18	310
Zr	216	228	91	115	130	204	12	8	15	22	22	21	400	38	218

paleo: paleosol, calcr: calcrete, fluv: fluvial, diat s: diatomaceous sediments, carb: carbonate, pyroc: pyroclastic.
* Data sources: Viereck-Götte (pers. comm., 2004).

smectite, smaller amounts of illite, locally kaolinite, and sepiolite, accompanied mainly by feldspar, quartz, calcite, opal-CT, pyroxene and, locally, trace amounts of gypsum. Smectite predominates mainly in the paleosol and calcrete levels in the volcano-sedimentary profile of the İncesu and Güzelöz districts.

Partial to complete alteration of plagioclase, K-feldspar, and pyroxene, partial devitrification of glass-shard particles in pyroclastic rocks, development of microsparitic to sparitic cement comprising euhedral rhombic calcite crystals between irregular clay nodules in paleosol and calcrete samples, as well as the occurrence of dogtooth-type sparitic crystals as fillings in fractures, desiccation cracks and geopetal-type fenestrae, indicate an alternation of drought and wet periods, resulting in development of paleosols and calcretes (Scholle, 1978; Wright *et al.*, 1988; Tucker and Bathurst, 1990; Wright and Tucker, 1991).

The association of smectite with mainly feldspar, pyroxene and traces of opal-CT, and micromorphological development of spongiform smectite on relict feldspar and, locally, glass shards indicate an authigenic origin. Thus, the smectite originated from precursor pyroclastic minerals such as feldspar, pyroxene and opal-CT.

The dissolution of feldspar, and volcanic glass shards, under conditions of low drainage or stagnant pore or connate water, supplied significant Si and Al for smectite precipitation. The immobility to low mobility of Al and Si, and low flushing of water in a stagnant environment, resulted in an alkaline environment favorable for the development of authigenic spongiform smectite on feldspar and glass shards (Kadir and Karakaş, 2002). Similar concentration of Al and Si may have resulted in the precipitation of kaolinite where drainage was high, resulting in an acidic environmental situation due to the leaching of mobile elements (such as K, Na and Ca) in kaolinite-bearing levels (Arslan *et al.*, 2006). A gradual reduction of Al and an increase of Mg following precipitation of smectite favor local precipitation of trace quantities of sepiolite (Singer and Galán, 1984; Akbulut and Kadir, 2003). Dissolution of feldspar may result in excess K and Al causing precipitation of illite authigenically or conversion of smectite to illite-

smectite (Hower *et al.*, 1976; Bethke and Altaner, 1986; Rask *et al.*, 1997). Therefore, the availability of K has been the controlling factor in the precipitation of illite rather than smectite. Authigenic quartz and opal-CT developed from excess silica following precipitation of neoformed clay minerals and degradation of diatoms.

CONCLUSIONS

In the Güzelöz area, lake water is found to be shallow and fluctuated, whereas in the İncesu area, lake water was comparatively deeper. Thus, diatomites occur as thin laminated beds. In addition, limestone levels occur interbedded with diatomites indicating change in climate. Pliocene paleosols are reported for the first time in the region of CVP and classified as Histosol, Aridisol and Alfisol. Smectite developed authigenically by the degradation of feldspar, pyroxene and the devitrification of volcanic glass driven by water flux in a shallow paleoenvironmental situation of paleosol and calcrete. Illite could have been formed by either direct precipitation, or by conversion of smectite to illite-smectite in the presence of K in the environment.

ACKNOWLEDGMENTS

This study was supported financially by the Scientific and Technical Research Council of Turkey (TÜBİTAK) in the framework of Project No. 104Y070. The authors are greatly indebted to Dr Warren Huff and anonymous reviewers for their critical reviews and suggestions which improved the manuscript. We are also extremely grateful to Dr Derek C. Bain for his editorial comments and suggestions. Dr Bekir N. Altın and Dr Cengiz Kayacılar are thanked for their help in preparing the geomorphological map.

REFERENCES

Akbulut, A. and Kadir, S. (2003) The geology and origin of sepiolite, palygorskite and saponite in Neogene lacustrine sediments of the Serinhisar-Acıpayam basin, Denizli, SW Turkey. *Clays and Clay Minerals*, **51**, 279–292.

Arslan, M., Kadir, S., Abdioğlu, E. and Kolayli, H. (2006) Origin and formation of kaolin minerals in saprolite of Tertiary alkaline volcanic rocks, Eastern Pontides, NE Turkey. *Clay Minerals*, **41**, 597–617.

Batum, I. (1975) Petrographische und geochemische Untersuchungen in den Vulkangebieten Göllü Dağ und Acıgöl (Zentralanatolien/Türkei). PhD thesis, Freiburg University, Germany, 101 pp.

Batum, I. (1978) Geology and petrography of the Göllüdağ and Acıgöl volcanics in the southwestern Nevşehir. *Bulletin of Earth Sciences Application and Research Centre of Hacettepe University*, Ankara, Turkey, **4/1-2**, 50–69 (in Turkish with English abstract).

Besang, C., Eckhardt, F.J., Harre W., Kreuzer, H. and Müller, P. (1977) Radiometrische Altersbestimmungen an Neogenen eruptivgesteinen der Turkei. *Geologisches Jahrbuch*, **B25**, 3–36.

Bethke, C.M. and Altaner, S.P. (1986) Layer-by-layer mechanism of smectite illitization and application to a new rate law. *Clays and Clay Minerals*, **34**, 136–145.

Bigazzi, G., Yeğingil, Z., Boztuğ, D., Ercan, T., Norelli, P. and Özdoğan, M. (1997) Studi di Proveinenza della obsidiana con il metodo tracce di fissione: nuovi dati sulle Potenziali fonti Anatoliche. *IV Giornata 'Le Scienze della Terra e l' Archeometria', Naples*, Abstracts, p. 33.

Brindley, G.W. (1980) Quantitative X-ray analysis of clays. Pp. 411–438 in: *Crystal Structures of Clay Minerals and their X-ray Identification* (G.W. Brindley and G. Brown, editors). Mineralogical Society Monograph 5, London.

Duritt, T.H., Brenchley, P.J., Gökten, Y.E. and Francaviglia, V. (1995) Late Quaternary rhyolitic eruptions from the Acıgöl complex, Central Turkey. *Journal of the Geological Society, London*, **152**, 655–667.

Ercan, T., Köse, C., Akbaşlı, A. and Yıldırım, T. (1987) Orta Anadolu'da Nevşehir-Niğde-Konya dolayındaki volkanik kökenli gaz çıkış
ları. *Cumhuriyet Üniversitesi Mühendislik Fakültesi Dergisi, Seri A, Yerbilimleri*, **4**, 57–63.

Ercan, T., Yeğingil, Z. and Biggazi, G. (1989) Obsidiyen tanımı ve özellikleri, Anadolu'daki dağılımı ve Orta Anadolu obsidiyenlerinin jeokimyasal nitelikleri. *Jeomorfoloji Dergisi*, **17**, 71–83.

Erol, O. (1999) A geomorphological study of the Sultansazliği lake, central Anatolia. *Quaternary Science Reviews*, **18**, 647–657.

Gabriel, M. and Malecha, A. (1972) *Evaluation of diatomite deposits near Belisırma and Ihlara and of occurences near Ürgüp (Niğde) and Çerke*ş (Çankırı) Turkey. The Etibank Rapport, (unpublished) Ankara, 17 pp..

Galán, E. and Ferrero, A. (1982) Palygorskite-sepiolite clays of Lebrija, southern Spain. *Clays and Clay Minerals*, **30**, 191–199.

Gevrek, A.İ. (1997) Aksaray doğusu, Ihlara-Derinkuyu yöresindeki volkaniklastiklerin sedimentolojisi. Doktora Tezi, A. Ü. Fen Bilimleri Enstitüsü 178 pp (in Turkish).

Göncüoğlu, M.C. and Toprak, V. (1992) Neogene and Quaternary volkanism of Central Anatolia: a volcano structural evoluation. *Bulletin de la Section de Volcanologie, Societè Geologique de France*, **26**, 1–6.

Hay, R.L. and Reeder, R.J. (1978) Calcretes of Olduvai Gorge and the Ndolanya Beds of northern Tanzania. *Sedimentology*, **25**, 649–673.

Henderson, J.H., Jackson, M.L., Syers, J.K., Clayton, R.N. and Rex, R.W. (1971) Cristobalite authigenic origin in bentonites. *Clays and Clay Minerals*, **19**, 229–238.

Hower, J., Eslinger, E.V., Hower, M. and Perry, E.A. (1976) Mechanism of burial metamorphism of argillaceous sediments, I. Mineralogical and chemical evidence. *Geological Society of American Bulletin*, **87**, 725–737.

Iijima, A. (1980) Geology of natural zeolites and zeolitic rocks. Pp. 103–118 in: *Proceedings of the 5th International Conference on Zeolites, Naples*, vol. 1. Heyden, London.

Iijima, A. and Tada, R. (1981) Silica diagenesis of Neogene diatomaceous and volcaniclastic sediments in northern Japan. *Sedimentology*, **28**, 185–200.

Innocenti, F., Mazzuoli, G., Pasquaré, F., Radicati Di Brozolo, F. and Villari, L. (1975) The Neogene calcalkaline volcanism of Central Anatolia – geochronological data on Kayseri-Niğde area. *Geological Magazine*, **112**, 349–360.

Jones, J.B. and Segnit, E.R. (1971) The nature of opal I. Nomenclature and constituent phases. *Journal of the Geological Society of Australia*, **18**, 57–68.

Kadir, S. and Karakaş, Z. (2002) Mineralogy, chemistry and origin of halloysite, kaolinite and smectite from Miocene ignimbrites, Konya, Turkey. *Neues Jahrbuch für Mineralogie, Abhandlungen*, **177**, 113–132.

Kadir, S., Baş, H. and Karakaş, Z. (2002) Origin of sepiolite and loughlinite in a Neogene sedimentary lacustrine environment, Mihalıçık-Eskişehir, Turkey. *The Canadian Mineralogist*, **40**, 1091–1102.

Karakaş, Z. and Kadir, S. (1998) Mineralogical and genetic relationships between carbonate and sepiolite-palygorskite formations in the Neogene lacustrine Konya Basin, Turkey. *Carbonates and Evaporites*, **13**, 198–206.

Kastner, M. (1979) Silica polymorphs. Pp. 99–106 in: *Marine Minerals* (R.G. Burns, editor). Short Course Notes, **6,** Mineralogical Society of America, Washington D.C.

Le Pennec, J.L., Bourdier, J.L., Froger, A., Temel, A., Camus, G. and Gourgaud, A. (1994) Neogene ignimbrites of the Nevşehir Plateau (central Turkey): stratigraphy, distribution and source constrains. *Journal of Volcanology and Geothermal Research*, **63**, 59–87.

Le Pennec, J.L., Temel, A., Froger, J.L., Sen, S.G., Gourgaud, A. and Bourdier, J.L. (2005) Stratigraphy and age of the Cappadocia ignimbrites, Turkey: reconciling field constraints with paleontologic, radiochronologic, geochemical and paleomagnetic data. *Journal of Volcanology and Geothermal Research*, **141**, 45–64.

Miall, A.D. (1996) *The Geology of Fluvial Deposits. Sedimentary Facies, Basin Analysis, and Petroleum Geology*. Springer, Berlin, 582 pp.

Moore, D.M. and Reynolds, R.C. (1989) *X-ray Diffraction and the Identification and Analysis of Clay Minerals*. Oxford University Press, New York, 332 pp.

MTA (1989) *1/100,000 Scale Geological Map of Turkey Kayseri-I19*. The General Directorate of Mineral Research and Exploration of Turkey.

Noel, D. (1984) Les diatomèes des scumures et des sediménts de surface du Salin de Bros del port (Santa pola province d'Alicante, Espagne). *Revista Instituto Investigaciones Geologicas, Barcelona*, **38-39**, 79–107.

Pasquaré, G. (1968) Geology of the Cenozoic volcanic area of Central Anatolia. *Atti Accademei Nazionale dei Lincei Memoire*, **9**, 55–204.

Pasquaré, G., Poli, S., Venzolli, L. and Zanchi, A. (1988) Continental arc volcanism and tectonic setting in Central Anatolia, Turkey. *Tectonophysics*, **146**, 217–230.

Rask, J.H., Bryndzıa, L.T., Braunsdorf, N.R. and Murray, T.E. (1997) Smectite illitization in Pliocene-age Gulf of Mexico mudrocks. *Clays and Clay Minerals*, **45**, 99–109.

Retallack, G.J. (1988) Field recognition of paleosols. Pp. 1–20 in: *Paleosols and Weathering through Geologic Time Techniques and Applications* (J. Reinhardt and W.R. Sigleo, editors). Special Paper, **216**, Geological Society of America, Boulder, Colorado.

Riding, R. and Wright, V.P. (1981) Paleosols and tidal flat-lagoon sequences on a Carboniferous carbonate shelf. *Journal of Sedimentary Petrology*, **51**, 1323–1339.

Scholle, P.A. (1978) A color illustrated guide to carbonate rock constituents, textures, cements and porosities. *Memoirs of the American Association of Petroleum Geology*, **27**, 241.

Schreiber, B.C. and El Tabakh, M. (2000) Deposition and early alteration of evaporites. *Sedimentology*, **47**, 215–238.

Schumacher, R., Keller, J. and Bayhan, H. (1990) Depositional characteristics of ignimbrites in Cappadocia, Central Anatolia, Turkey. Pp. 435–449 in: *Proceedings of the International Earth Science Congress on Aegean Regions (IESCA-1990)*, vol. **2** (M.Y. Savaşçın and A.H. Eronat, editors).

Schumacher, R. and Schumacher, U.M. (1996) The Kızılkaya ignimbrite an unusual low-aspect-ratio ignimbrite from Cappadocia, Central Turkey. *Journal of Volcanolgy and Geothermal Rescarch*, **70**, 107–121.

Siesser, W.G. (1973) Diagenetically formed ooids and intraclasts in South African calcretes. *Sedimentology*, **20**, 539–551.

Singer, A. and Galán, E., editors (1984) *Palygorskite-Sepiolite; Occurrence, Genesis and Uses*. Development in Sedimentology, **37**, Elsevier, Amsterdam, 352 pp.

Stamatakis, M.G., Hein, J.R. and Magganas, A.C. (1989) Geochemistry and diagenesis of Miocene lacustrine siliceous sedimentary and pyroclastic rocks, Mytilinii basin, Greece. *Sedimentary Geology*, **64**, 65–78.

Temel, A., Gündoğdu, M.N., Gourgaud, A. and Le Pennec, J.L. (1998) Ignimbrites of Cappadocia Central Anatolia, Turkey: petrology and geochemistry. *Journal of Volcanology and Geothermal Research*, **85**, 447–471.

Toprak, V., Keller, J. and Schumacher, R. (1994) Volcano-tectonic features of the Cappadocian Volcanic Province. *International Volcanological Congress*, *Excursion Guide*, Ankara, 58 pp.

Toprak, V. (1996) *The origin of the Quaternary basins which have been developed in the Cappadocia volcanic subsidence, Central Anatolia*. 30th annual symposium, Black Sea Technical University, Trabzon (in Turkish), pp. 326–340.

Tucker, M.E. and Bathurst, R.G.C. (1990) *Carbonate Diagenesis*. Blackwell Scientific Publications, Oxford, UK, **1**, 312 pp.

Türkecan, A., Dönmez, M. and Akçay, E.A. (2003) *Tertiary volcanics of Kayseri-Niğde-Nevşehir* areas. Mineral Research and Exploration Report, no. 10575 (unpublished), Ankara (in Turkish).

Uygun, A. (1976) Geologie und Diatomit Vorkommen des Neogen-Beckens von Emmiler-Hırka (Kayseri-Türkei), PhD thesis, Bonn Universitaet, Germany, 137 pp.

Viereck-Götte, L. and Gürel, A. (2003) Klima- und Vegetationswechsel dokumentiert in Obermiozaenen Paläoböden Kappadokiens, Zentralanatolien. *Berichte der Deutschen Mineralogischen Gesellschaft. Beihefte zum European Journal of Mineralogy*, **15**, 211 pp., Stuttgart, Germany.

Warren, J.K. (1982a) The hydrological significance of Holocene tepees, stromatolites, and boxwork limestones in coastal salines in South Australia. *Journal of Sedimentary Petrology*, **52**, 1171–1201.

Warren, J.K. (1982b) The hydrological setting, occurrence and significance of gypsum in late Quaternary salt lakes in South Australia. *Sedimentology*, **29**, 609–637.

Wright, V.P. (1982) Calcrete paleosol from Carboniferous Llanelli Formation, South Wales. *Sedimentary Geology*, **33**, 1–33.

Wright, V.P. (1983) A rendzina from the Lower Carboniferous of South Wales. *Sedimentology*, **30**, 159–179.

Wright, V.P. (1986) The role of fungal biomineralization in the formation of Early Carboniferous soil fabrics. *Sedimentology*, **33**, 831–838.

Wright, V.P. (1987) The ecology of two early Carboniferous paleosols: Pp. 345–358 in: *European Dinantian Environments* (J. Miller, A.E. Adams and V.P. Wright, editors). Geological Journal Special Issue, **12**, Wiley, London.

Wright, V.P. and Tucker, M.E. (1991) *Calcretes*. The International Association of Sedimentologists, Oxford, London, 352 pp.

Wright, V.P., Platt, N.H. and Wimbledon, W.A. (1988) Biogenic laminar calcretes: evidence of calcified root-mat horizons in paleosols. *Sedimentology*, **35**, 603–620.

(*Received 28 June 2005; revised 3 April 2006; Ms. 1065; A.E. Warren D. Huff*)